

[Article]

DOI: 10.13208/j.electrochem.201243

Http://electrochem.xmu.edu.cn

Electrochemical Gating Single-Molecule Circuits with Parallel Paths

Jun-Qing Su^{1#}, Yi-Fan Zhou^{1#}, Ling Tong¹, Ya-Hao Wang¹,
Ju-Fang Zheng¹, Jing-Zhe Chen², Xiao-Shun Zhou^{1*}

(1. Key Laboratory of the Ministry of Education for Advanced Catalysis Materials, Institute of Physical Chemistry, Zhejiang Normal University, Jinhua 321004, Zhejiang, China; 2. Department of Physics, Shanghai University, Shanghai 200444, China)

Abstract: Electrochemical gating has emerged as a feasible and powerful method to tune single-molecule conductance. Herein, we demonstrate that the electron transport through single-molecule circuits with two benzene rings in parallel could be efficiently gated by electrochemistry. The molecular junctions with two parallel paths are fabricated with Au electrodes by STM break junction (STM-BJ) technique. Their conductance value exhibits a 2.82-fold enhancement by the constructive quantum interference compared to single-molecule junctions with single path for electron tunneling. Furthermore, the conductance of para-benzene based molecule could be electrochemically tuned with a modulation ratio of about 333% · V⁻¹. With the help of DFT calculations, a V-shape spectra of energy-dependent transmission coefficients $T(E)$ around $E = E_F$ leads to the conductance gating behavior. The current work sheds a light on the electrochemical gating of single-molecule circuits with parallel paths, and offers a new way to design molecular materials for a high-performance molecular device.

Key words: molecular junctions; electrochemical gating; molecular structure; ECSTM-BJ; constructive quantum interference

1 Introduction

Tuning electron transport through metal-molecule-metal junctions is significant step forward realizing single-molecule switch and transistor^[1]. During past two decades, external stimulus, such as pH^[2,3], light^[4-6], magnetism^[7] and electricity^[8,9], have been used to achieve this goal. Among them, electrochemistry offers a feasible method to tune the electron transport at the single-molecular scale by shifting the Fermi level of two work electrodes (source and drain)^[10-13]. Typically, redox-active molecules, including ferrocene^[14-18], anthraquinone^[19,20], and viologen^[21], that could transform between the oxidation and reduction

states upon electrochemical potentials, have been widely investigated to illustrate the electrochemical gating at single molecular level. For non-redox molecules, however, rare cases have been reported^[22,23], which heavily limits the application of electrochemical gating.

To solve above problems, optimizing the molecular structure recently has been explored to activate electrochemical gating behavior^[24] or generate electrochemically-controlled quantum interference^[25-27]. For example, a fused molecular structure consisting of selenophene rings of shows one order magnitude of conductance modulation ratio within a potential

Citation: Su J Q, Zhou Y F, Tong L, Wang Y H, Zheng J F, Chen J Z, Zhou X S. Electrochemical gating single-molecule circuits with parallel paths. *J. Electrochem.*, 27(2): 195-201.

Received: 2021-01-13, Revised: 2021-02-11. #These authors contributed equally to this work. *Corresponding author, Tel: (86-579) 82286876; E-mail: xszhou@zjnu.edu.cn

Financial support from the National Natural Science Foundation of China (No. 21872126,) and the Zhejiang Provincial Natural Science Foundation of China (No. LQ21B030010).

window of 1.2 V^[24]. Two orders of magnitude conductance minimum is observed at specific electrochemical potential for meta-benzene and 2,4-linkedthiophene derivatives with destructive quantum interference^[27]. These significant results reveal the intrinsic structure of molecule plays a key role in electrochemical gating of electron transport. Therefore, much more attention should be paid to investigate the impact of molecular structure on electrochemical gating.

Herein, we have fabricated the molecular junctions of a benzene derivative of 2,11-Dithia [3,3] paracyclophane (denoted as **M2**), consisting with two parallel CH₂-benzene-CH₂ units with terminal sulfur methyl groups, and measured its conductance. The conductance behavior depending on electrochemical gate potentials was measured by STM breaking junction technique in BMIPF₆. Compared to 1,4-bis(methylsulfanylmethyl)benzene with single path (denoted as **M1**), an obvious conductance modulation is observed for **M2**. With the help of calculated energy-dependent transmission spectra, the electrochemical gating mechanism is discussed.

2 Experimental Section

2.1 Single-Molecule Conductance Measurement

As schematically shown in Figure 1, conductance measurements by an electrochemical STM break-junction (ECSTM-BJ) setup are performed on a modified Nanoscope IIIa STM (Veeco, Plainview, NY, USA). Mechanically-cut Au tip (0.25 mm diameter, 99.99%, Alfa Assar) and Au (111) substrate are used as source and drain electrodes, respectively. According to previous report^[11], the Pt counter and Ag reference electrodes serve as a gate electrode. The electrochemical potentials of STM tip and substrate could be independently controlled by a bipotentiostat. The potential difference between the tip and substrate electrodes is the bias voltage applied to molecular junctions. In order to minimize Faraday current at few pA scales, Au tip is encapsulated by thermosetting polyethylene glue. The self-assembled monolayers (SAMs) of investigated molecules are papered in absolute ethyl al-

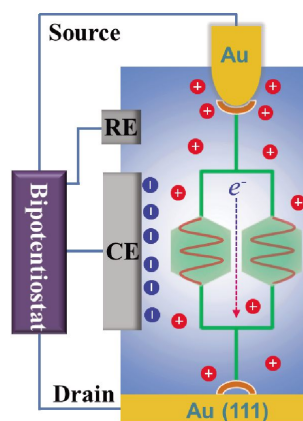


Figure 1 Schematic diagram of electrochemical gating electron transport through molecular junction with two parallel pathways. (color on line)

cohol solution containing 1 mmol·L⁻¹ target molecules. Before each experiment, BMIPF₆ was dried under vacuum at 70 °C for at least 12 hours to remove water and oxygen. All electrochemical STM experiments are carried out in N₂ atmosphere.

The brief protocol of ECSTM-BJ approach is described as follows. Firstly, the tip was driven toward the substrate to reach conductance value more than several G_0 . Then the tip was pulled away from the substrate at a constant speed of 20 nm·s⁻¹. During the process, the molecules with two terminal sulfur methyl groups could bridge between the broken Au atomic contacts to form single-molecule junction. Meanwhile, the current-distance curves were recorded at a sampling rate of 20 kHz. Thousands of those curves were collected to construct conductance histogram without any data selection.

2.2 Theoretical Calculation

The energy-dependent transmission spectra are calculated at the open-source package SHINE (Shanghai Integrated Numeric Engineering). The structure of the molecule junction is optimized until the maximum force on all the atoms is less than 0.05 eV·Å⁻¹. Perdew-Burke-Ernzerhof (PBE) functional is adopted for the exchange-correlation energy. For the sake of efficiency and accuracy, a single-zeta polarized (SZP) basis is adopted for electrodes, a double-zeta polarized (DZP) basis is adopted for molecule

part. Then the electron transmission is estimated using NEGF+DFT method, where the Hamiltonian of the system is constructed by DFT and electron density is calculated by NEGF formalism. A denser K-sampling (4×4) is used in the transverse plane.

3 Results and Discussion

3.1 Fabrication of Single-Molecule Circuits with Parallel Paths

The conductance measurements were first carried on the **M2** modified Au(111) in atmosphere environment to investigate the electron transport through a parallel path compared to **M1** with single path. Figure 2(A) shows the molecular structures of **M1** and **M2**. The obtained representative conductance-distance traces are displayed in Figure 2(B). Obviously, there are two step features at $10^{-3.3} G_0$ and $10^{-3.0} G_0$ for **M1**, and $10^{-2.55} G_0$ and $10^{-2.95} G_0$ for **M2**, respectively. This indicates there are two main configurations during the formation of single-molecule junctions. Thousands of these traces are collected to construct the one-dimensional conductance histograms without any data selection. As shown in Figure 2(C), two pronounced peaks located the step values in Figure 2(B) both for **M1** and **M2**. Similar to previous reports of $-\text{SCH}_3$ groups^[28-30], the two peak values at the most probable intensity in histogram is assigned to the single-molecule conductance and denote as high conductance (G_{HC}) and low conductance (G_{LC}) for two different configurations.

Quantitatively, the two sets of conductance values

of **M2** are significantly larger than those of **M1**. It's found that both the ratios of $G_{\text{LC}}(\mathbf{M2})/G_{\text{LC}}(\mathbf{M1})$ and $G_{\text{HC}}(\mathbf{M2})/G_{\text{HC}}(\mathbf{M1})$ are around 2.82. These interesting results are coincided with previous theoretical prediction and experimental results in literatures. And there is a constructive quantum interference as the electron transport through the single-molecule circuits with parallel paths^[28,31,32]. Thus, the total conductance of two parallel paths components with quantum interference effect does not obey traditional Kirchhoff's circuit law, and 2.82-fold conductance enhancement of **M2** is observed compared to that of **M1**.

3.2 Electrochemical Gating Measurement

Now we turn to investigate the electrochemical gating of single-molecule circuits with parallel paths in BMIPF₆. The ionic liquid is used as electrolyte to gate single-molecule conductance, because it could efficiently couple with applied electric field^[10]. The electrode potentials are individually controlled relative to Ag wire reference electrode while keep a fixed bias voltage of 50 mV ($E_{\text{tip}} - E_{\text{substrate}}$). Figure 3(A) shows the conductance histograms upon different gate potential of $E_{\text{substrate}}$. Interestingly, only one pronounced conductance peak is observed in BMIPF₆, which indicates that the solvent environment has an impact on the binding configurations of **M2**. It's reported that the imidazole ring of BMI cations could adsorb on Au^[33], which could generate a steric effect and an interfacial electronic effect to change the interaction of thiomethyl groups of **M2** on atomic-flat Au (111)

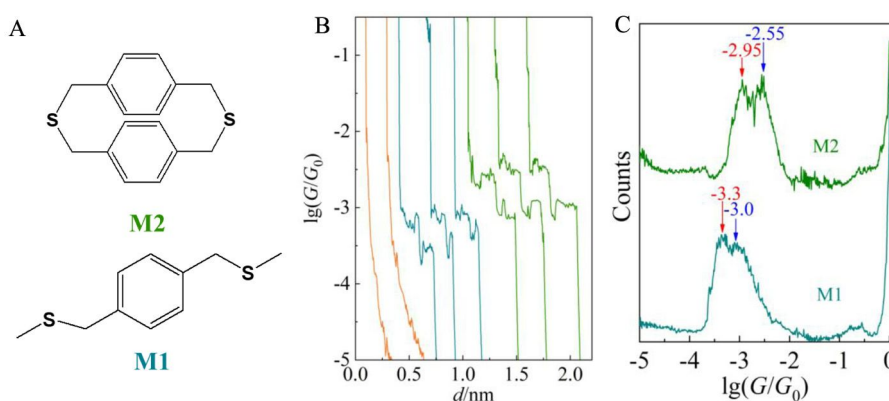


Figure 2 (A) The investigated molecular structures of **M1** and **M2**. (B) The typical conductance-distance curves and (C) 1D conductance histogram of **M1** (blue) and **M2** (green). Orange curves are exponential decay without molecular junction formation.(color on lin)

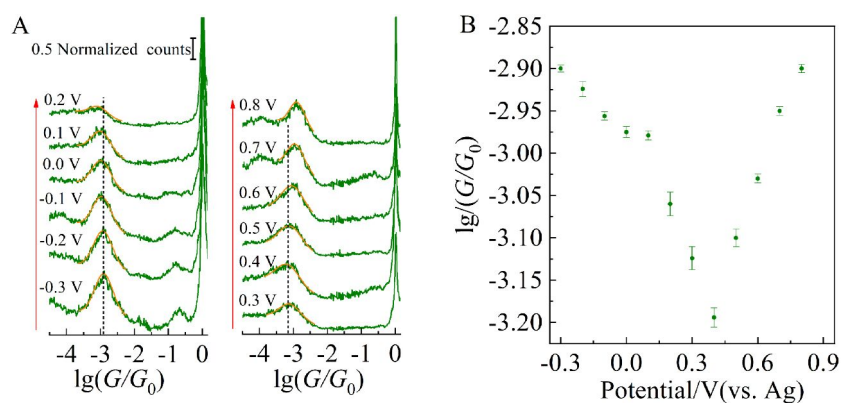


Figure 3 (A) Conductance histograms of **M2** at different gated potentials of $E_{\text{substrate}}$ from -0.3 V to 0.9 V. (B) The plot of experimentally measured conductance against the applied $E_{\text{substrate}}$. The conductance peak counts are normalized by the numbers of conductance curves used. (color on line)

surface. In addition, the two benzene rings are linked to each other through the $-\text{CH}_2\text{SCH}_2-$ groups attached to the para-positions. This could make the binding groups more rigid. Thus, **M2** is more susceptible to adsorption of BMI cations in the solvent compared to **M1**.

As $E_{\text{substrate}}$ increases from -0.3 V to 0.8 V, the conductance values of **M2** in Figure 3(A) first decrease from $10^{-2.90} G_0$ to $10^{-3.17} G_0$, and reaches a minimum at 0.4 V. Then the peak values increase to $10^{-2.90} G_0$ at 0.9 V, giving out a modulation ratio of about 200% as the gate potential changes 0.6 V ($333\% \cdot \text{V}^{-1}$). We have also performed electrochemical gating of **M1** at the same experimental conditions. The maximum conductance gating ratio is only about 25% for **M1** (Figure S1). This lack of significant gate effect is attributed to the larger LUMO-HOMO gaps of **M1** (5.2 eV) compared to that of **M2** (-4.8 eV) (details in Figure S2). Thus, **M2** with two parallel paths for electron transport significantly improve electrochemical gating efficiency, and provides a feasible way to design of high-performance molecular switch and transistors.

3.3 Theoretical Analysis

For electrochemical gating, the main feature is shifting the Fermi level of electrodes relative to the frontier orbitals of molecules by applying potential on electrode. As illustrated in Figure 4(A), the E_{F} of electrodes could increase as applied gate potentials

negatively shift and vice versa, which could change the energy alignment between the molecules and electrodes and tune the electron transport. To further clarify the gating mechanism of **M2**, we calculate the energy-dependent transmission spectra using nonequilibrium Green's function (NEGF)^[34,35]. The optimized configurations of molecular junctions in Figure 4B as relaxing the maximum atomic force less than $0.05 \text{ eV} \cdot \text{Å}^{-1}$. It's found that the molecule anchors to gold through S atoms in $-\text{SCH}_2-$ groups, and the Au-S bond length of 2.8 Å is obtained similar to the previous computed results^[36]. Figure 4(B) displays the transmission coefficients $T(E)$ of **M2** molecular junction depending on the energy level of molecular orbitals relative to Fermi level of electrode ($E-E_{\text{F}}$). Qualitatively, the $T(E)$ around $E = E_{\text{F}}$ shows a V-shape curve consistent with the gating behavior of measured conductance. In addition, it's reported that a destructive quantum interference (DQI) of electron transport through parallel para-benzene could be generated as modulating through-space coupling between benzene ring and electrode^[28]. And DQI could lead to more than two orders of magnitude conductance change in previous reports^[25,27]. Considering about a 200% modulation for **M2**, an "imperfect" DQI might also happen as the coupling between the benzene ring or anchoring group and electrode may be changed during electrochemical gating.

To quantitatively correlate the theoretical $T(E)$ and experimental conductance value, the E_{F} of Au sub

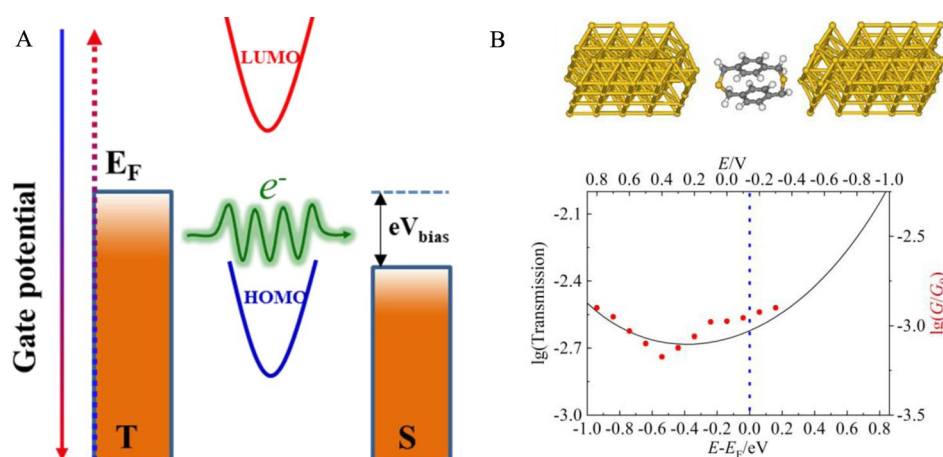


Figure 4 (A) The schematic diagram of electrochemical gating mechanism for **M2** molecular junctions in ILs (B) experimental (red circle) and calculated (black line) molecular conductance for **M2** as a function of the applied gating potential vs. Ag. The energy level of electrode at $(E - E_F) = 0$ (bottom x axis) is estimated to be -4.3 eV, which corresponds to the electrode potential of -0.14 V vs. Ag. Insert at top is the optimized geometries of molecular junction of **M2**. (color on line)

strate is estimated according to the formula: $E_F = -4.44 - E_{\text{potential}}$, where $E_{\text{potential}}$ is the applied potential of Au(111) substrate, -4.44 eV is the energy level of Ag reference electrode determined by using the redox potential of ferrocene (F_c^+/F_c) as a standard of -4.8 eV in BMIPF₆^[37] (details in Figure S3). Previous reports and the calculation results have confirmed that the work function of Au assembled with molecules is 4.3 eV^[27, 38]. Therefore, the electrode potential is calculated to be -0.14 V vs. Ag at $E = E_F$. And the experimental conductance values at different gate potentials are well correlated to theoretical $T(E)$.

4 Conclusions

In summary, the molecular junctions of **M2** with two parallel paths have been fabricated with Au electrodes by STM-BJ and measured their conductance. A constructive quantum interference of electron transport is observed in single-molecule circuits two parallel paths, which leads to 2.82-fold conductance value compared to that of **M1** with single path. Furthermore, the conductance of **M2** could be electrochemically tuned with a modulation ratio of about $333\% \cdot V^{-1}$. The combined DFT calculations reveals that the significant conductance gating behavior in well coincide with the energy-dependent transmission coefficients $T(E)$. The current work proves that

the molecules with two parallel paths can greatly improve the electrochemically gating performance, and provides a new way to design a high-performance molecular device.

Supporting Information

Additional information as noted in text. This material is available free of charge via the internet at <http://electrochem.xmu.edu.cn>.

References:

- [1] Xiang D, Wang X L, Jia C C, Lee T, Guo X F. Molecular-scale electronics: from concept to function[J]. Chem. Rev., 2016, 116(7): 4318-4440.
- [2] Brooke R J, Szumski D S, Vezzoli A, Higgins S J, Nichols R J, Schwarzacher, W. Dual control of molecular conductance through pH and potential in single-molecule devices[J]. Nano Lett., 2018, 18(2): 1317-1322.
- [3] Li Z H, Smeu M, Afsari S, Xing Y J, Ratner M A, Borguet E. Single-molecule sensing of environmental pH-an STM break junction and NEGF-DFT approach[J]. Angew. Chem. Int. Ed., 2014, 53(4): 1098-1102.
- [4] Cai S N, Deng W T, Huang F F, Chen L J, Tang C, He W X, Long S C, Li R H, Tan Z B, Liu J Y, Shi J, Liu Z T, Xiao Z Y, Zhang D Q, Hong W J. Light-driven reversible intermolecular proton transfer at single-molecule junctions[J]. Angew. Chem. Int. Ed., 2019, 58(12): 3829-3833.
- [5] Jia C C, Migliore A, Xin N, Huang S Y, Wang J Y,

- Yang Q, Wang S P, Chen H L, Wang D M, Feng B Y, Liu Z R, Zhang G Y, Qu D H, Tian H, Ratner M A, Xu H Q, Nitzan A, Guo X F. Covalently bonded single-molecule junctions with stable and reversible photoswitched conductivity-SM[J]. *Science*, 2016, 352(6292): 1443-1445.
- [6] Sendler T, Luka-Guth K, Wieser M, Lokamani Wolf J, Helm M, Gemming S, Kerbusch J, Scheer E, Huhn T, Erbe A. Light-induced switching of tunable single-molecule junctions[J]. *Adv. Sci.*, 2015, 2(5): 1500017.
- [7] Mannini M, Pineider F, Danieli C, Totti F, Sorace L, Sainctavit P, Arrio M A, Otero E, Joly L, Cezar J C, Cornia A, Sessoli R. Quantum tunnelling of the magnetization in a monolayer of oriented single-molecule magnets[J]. *Nature*, 2010, 468(7322): 417-421.
- [8] Kay N J, Higgins S J, Jeppesen J O, Leary E, Lycoops J, Ulstrup J, Nichols R J. Single-molecule electrochemical gating in ionic liquids[J]. *J. Am. Chem. Soc.*, 2012, 134(40): 16817-16826.
- [9] Song H, Kim Y, Jang Y H, Jeong H, Reed M A, Lee T. Observation of molecular orbital gating[J]. *Nature*, 2009, 462(7276): 1039-1043.
- [10] Huang C C, Rudnev A V, Hong W J, Wandlowski T. Break junction under electrochemical gating: testbed for single-molecule electronics[J]. *Chem. Soc. Rev.*, 2015, 44(4): 889-901.
- [11] Osorio H M, Catarelli S, Cea P, Gluyas J B G, Hartl F, Higgins S J, Leary E, Low P J, Martin S, Nichols R J, Tory J, Ulstrup J, Vezzoli A, Milan D C, Zeng Q. Electrochemical single-molecule transistors with optimized gate coupling[J]. *J. Am. Chem. Soc.*, 2015, 137(45): 14319-14328.
- [12] Díez-Pérez I, Li Z H, Guo S Y, Madden C, Huang H L, Che Y K, Yang X M, Zang L, Tao N J. Ambipolar transport in an electrochemically gated single-molecule field-effect transistor[J]. *ACS Nano*, 2012, 6(8): 7044-7052.
- [13] Ramachandran R, Li H B, Lo W Y, Neshchadin A, Yu L P, Hihath J. An electromechanical approach to understanding binding configurations in single-molecule devices[J]. *Nano Lett.*, 2018, 18(10): 6638-6644.
- [14] Zhou X S, Liu L, Fortgang P, Lefevre A S, Serra-Muns A, Raouafi N, Amatore C, Mao B W, Maisonhaute E, Schollhorn B. Do molecular conductances correlate with electrochemical rate constants? Experimental insights[J]. *J. Am. Chem. Soc.*, 2011, 133(19): 7509-7516.
- [15] Sun Y Y, Peng Z L, Hou R, Liang J H, Zheng J F, Zhou X Y, Zhou X S, Jin S, Niu Z J, Mao B W. Enhancing electron transport in molecular wires by insertion of a ferrocene center[J]. *Phys. Chem. Chem. Phys.*, 2014, 16(6): 2260-2267.
- [16] Yuan Y, Yan J F, Lin D Q, Mao B W, Yuan Y F. Ferrocene-alkynyl conjugated molecular wires: synthesis, characterization, and conductance properties[J]. *Chem.-Eur. J.*, 2018, 24(14): 3545-3555.
- [17] Xiao X Y, Brune D, He J, Lindsay S, Gorman C B, Tao N J. Redox-gated electron transport in electrically wired ferrocene molecules[J]. *Chem. Phys.*, 2006, 326(1): 138-143.
- [18] Zhang F, Wu X H, Zhou Y F, Wang Y H, Zhou X S, Shao Y, Li J F, Jin S, Zheng J F. Improving gating efficiency of electron transport through redox-active molecular junctions with conjugated chains[J]. *ChemElectroChem*, 2020, 7(6): 1337-1341.
- [19] Darwish N, Díez-Pérez I, Guo S Y, Tao N J, Gooding J J, Paddon-Row M N. Single molecular switches: electrochemical gating of a single anthraquinone-based norbornylogous bridge molecule[J]. *J. Phys. Chem. C*, 2012, 116(39): 21093-21097.
- [20] Darwish N, Díez-Pérez I, Da S P, Tao N J, Gooding J J, Paddon-Row M N. Observation of electrochemically controlled quantum interference in a single anthraquinone-based norbornylogous bridge molecule[J]. *Angew. Chem. Int. Ed.*, 2012, 51(13): 3203-3206.
- [21] Haiss W, van Zalinge H, Higgins S J, Bethell D, Hobenreich H, Schiffrin D J, Nichols R J. Redox state dependence of single molecule conductivity[J]. *J. Am. Chem. Soc.*, 2003, 125(50): 15294-15295.
- [22] Capozzi B, Chen Q, Darancet P, Kotiuga M, Buzzeo M, Neaton J B, Nuckolls C, Venkataraman L. Tunable charge transport in single-molecule junctions via electrolytic gating[J]. *Nano Lett.*, 2014, 14(3): 1400-1404.
- [23] Baghernejad M, Manrique D Z, Li C, Pope T, Zhumaev U, Pobelov I, Moreno-Garcia P, Kaliginedi V, Huang C, Hong W J, Lambert C, Wandlowski T. Highly-effective gating of single-molecule junctions: an electrochemical approach[J]. *Chem. Commun.*, 2014, 50(100): 15975-15978.
- [24] Wang Y H, Yan F, Li D F, Xi Y F, Cao R, Zheng J F, Shao Y, Jin S, Chen J Z, Zhou X S. Enhanced gating performance of single-molecule conductance by heterocyclic molecules[J]. *J. Phys. Chem. Lett.*, 2021, 12(2): 758-763.
- [25] Bai J, Daaoub A, Sangtarash S, Li X H, Tang Y X, Zou Q, Sadeghi H, Liu S, Huang X J, Tan Z B, Liu J Y, Yang Y, Shi J, Meszaros G, Chen W B, Lambert C, Hong W J. Anti-resonance features of destructive quantum interference in single-molecule thiophene junctions achieved by electrochemical gating[J]. *Nat. Mater.*, 2019, 18(4): 364-369.
- [26] Li Y Q, Buerkle M, Li G F, Rostamian A, Wang H, Wang

- Z X, Bowler D R, Miyazaki T, Xiang L M, Asai Y, Zhou G, Tao N J. Author correction: gate controlling of quantum interference and direct observation of anti-resonances in single molecule charge transport[J]. *Nat. Mater.*, 2020, 19(1): 127.
- [27] Huang B, Liu X, Yuan Y, Hong Z W, Zheng J F, Pei L Q, Shao Y, Li J F, Zhou X S, Chen J Z, Jin S, Mao B W. Controlling and observing sharp-valleyed quantum interference effect in single molecular junctions[J]. *J. Am. Chem. Soc.*, 2018, 140(50): 17685-17690.
- [28] Borges A, Xia J L, Liu S H, Venkataraman L, Solomon G C. The role of through-space interactions in modulating constructive and destructive interference effects in benzene[J]. *Nano Lett.*, 2017, 17(7): 4436-4442.
- [29] Tao C P, Jiang C C, Wang Y H, Zheng J F, Shao Y, Zhou X S. Single-molecule sensing of interfacial acid-base chemistry[J]. *J. Phys. Chem. Lett.*, 2020, 11(23): 10023-10028.
- [30] Kiguchi M, Ohto T, Fujii S, Sugiyasu K, Nakajima S, Takeuchi M, Nakamura H. Single molecular resistive switch obtained via sliding multiple anchoring points and varying effective wire length[J]. *J. Am. Chem. Soc.*, 2014, 136(20): 7327-7332.
- [31] Vazquez H, Skouta R, Schneebeli S, Kamenetska M, Breslow R, Venkataraman L, Hybertsen M S. Probing the conductance superposition law in single-molecule circuits with parallel paths[J]. *Nat. Nanotech.*, 2012, 7(10): 663-667.
- [32] Wang Y H, Li D F, Hong Z W, Liang J H, Han D, Zheng J F, Niu Z J, Mao B W, Zhou X S. Conductance of alkyl-based molecules with one, two and three chains measured by electrochemical STM break junction [J]. *Electrochem. Commun.*, 2014, 45: 83-86.
- [33] Zhang M, Yu L J, Huang Y F, Yan J W, Liu G K, Wu D Y, Tian Z Q, Mao B W. Extending the shell-isolated nanoparticle-enhanced Raman spectroscopy approach to interfacial ionic liquids at single crystal electrode surfaces[J]. *Chem. Commun.*, 2014, 50(94): 14740-14743.
- [34] Taylor J, Guo H, Wang J. Ab initio modeling of quantum transport properties of molecular electronic devices [J]. *Phys. Rev. B*, 2001, 63(24): 245407.
- [35] Chen J Z, Thygesen K S, Jacobsen K W. Ab initio nonequilibrium quantum transport and forces with the real-space projector augmented wave method[J]. *Phys. Rev. B*, 2012, 85(15): 155140.
- [36] Liu C Y, Wang H F, Ren Z G, Braunstein P, Lang J P. Fine-tuning of luminescence through changes in Au-S bond lengths as a function of temperature or solvent [J]. *Inorg. Chem.*, 2019, 58(13): 8533-8540.
- [37] Pommerehne J, Vestweber H, Guss W, Mahrt R F, Bässler H, Porsch M, Daub J. Efficient two layer LEDs on a polymer blend basis[J]. *Adv. Mater.*, 1995, 7(6): 551-554.
- [38] Low J Z, Capozzi B, Cui J, Wei S J, Venkataraman L, Campos L M. Tuning the polarity of charge carriers using electron deficient thiophenes[J]. *Chem. Sci.*, 2017, 8(4): 3254-3259.

电化学门控调节具有平行路径的单分子电路中电子传输

苏俊青^{1#}, 周一帆^{1#}, 童凌¹, 王亚浩¹, 郑菊芳¹, 陈竞哲², 周小顺^{1*}

(1. 浙江师范大学物理化学研究所, 先进催化材料教育部重点实验室, 浙江 金华 321004;

2. 上海大学物理系, 上海 200444)

摘要: 电化学门控已成为一种可行且高效调节单分子电导的方法。在本研究中, 我们证实了具有两个平行苯环的单分子电路中电子传输可以通过电化学门控控制。首先, 我们利用 STM-BJ 技术以金为电极构筑了具有两条平行路径的单分子结。与单条路径的单分子结相比, 两条路径的分子结由于具有增强性量子干涉效应, 具有 2.82 倍的电导值。进一步地, 我们利用电化学门控对具有两个平行苯环的单分子结的电导进行调控, 获得了 $333\% \cdot \text{V}^{-1}$ 调节比。结合 DFT 计算, 发现在 $E=E_F$ 附近的 V 形透射系数谱图导致了实验观测的电导门控行为。本研究揭示了具有平行路径的单分子电路的电化学门控行为, 并为设计高性能分子器件的分子材料提供了新的途径。

关键词: 分子结; 电化学门控; 分子结构; ECSTM-BJ; 增强性量子干涉